Korean J. Chem. Eng., **30**(8), 1578-1587 (2013)
DOI: 10.1007/s11814-013-0084-x

Application of real-time feedback control strategies based on effluent NH_4-N and NO_X-N concentrations in an A^2/O process

Hyosoo Kim*, Yejin Kim*, Trung Quang Hoang*, Gyeongdong Baek, Sungshin Kim***, and Changwon Kim*,†**

*Department of Civil and Environmental Eng., Pusan National University, Busan 609-735, Korea
**Daewoo Shipbuilding & Marine Engineering, Co., Ltd., Gyeonsangnam-do 656-714, Korea
***Department of Electrical Engineering, Pusan National University, Busan 609-735, Korea
(*Received 23 October 2012 • accepted 14 May 2013*)

Abstract−This paper proposes two real-time feedback control strategies based on hourly measurements of effluent NH_4-N and NO_X-N concentrations. Using modified sigmoid functions to decide the DO setpoint, a control structure similar to the cascade-type control loop was selected as the real-time feedback NH_4-N control strategy. For the real-time feedback NO_X-N control strategy, a proper external carbon dose flow rate could be calculated based on the estimated NO_X-N concentration in anoxic reactor by using the empirical equation. A control system, which included two proposed control strategies, was developed and applied in the pilot-scale A^2/O process. As a result, the effluent NH_4-N and NO_X-N concentrations were maintained stably lower than the target values of 3 and 5 mg/L, respectively. Moreover, because the manipulated variables for removing the NH_4-N and NO_X-N concentrations were divided in the control strategies, the two different control strategies could be successfully applied together in the A^2/O process.

Key words: Real-time Feedback NH_4-N Control Strategy, Real-time Feedback NO_X-N Control Strategy, Modified Sigmoid Function, Empirical Equation, A^2/O Process

INTRODUCTION

In a biological nutrient removal process, the nutrient removal performance should be managed consistently because the discharge of untreated nitrogen and phosphorus can cause the eutrophication of lakes, rivers and coasts [1]. In the case of phosphorous, it is difficult to achieve sufficient removal under a real-time control strategy. An effective manipulated variable for removal of a phosphorous component in biological nutrient removal process is the waste sludge flow rate, and a significant effect cannot be obtained quickly by changing the waste sludge flow rate. On the other hand, the manipulated variables for removal of NH_4-N and NO_X-N components are the DO, external carbon source and internal RAS flow rate, and the changes of their values can affect the process performance directly. Therefore, it can be possible to remove NH_4-N and NO_X-N by using a real-time control strategy.

Various studies related to the real-time control strategies for removing the NH_4-N and NO_X-N concentrations have been reported. Ingildsen et al. [2] investigated a real-time DO controller by using a simple hydraulic model based on ammonium sensor in källby WWTP for 100,000 PE. Krause et al. [3] compared pure feedback control with a configuration combining feedback and feedforward control, considering the influent ammonium load in full-scale WWTP. Vrečko et al. [4] tested and compared three different proportional integral (PI) controllers with control structures consisting of oxygen cascade, ammonia cascade and ammonia feedforward-cascade, respectively, and reported that the ammonia feedforward-cascade PI controller showed the best rejection performance of effluent ammonia peaks and 45% airflow saving. Moreover, the real-time control strategy was based on the knowledge-based expert system [5] and the dose of external carbon source was based on the mathematical model [6-8].

Although the NH_4-N concentration in an aerobic reactor and the NO_X-N concentration in an anoxic reactor could be controlled properly by using the aforementioned control structure, the effluent NH_4-N and NO_X-N concentrations might be degraded due to the change of settling ability in the secondary settler. Further, in South Korea, the effluent nitrogen concentrations are measured every hour and the measured concentrations are sent to the Ministry of Environment by TELE-monitoring system. The Ministry of Environment imposes a fine on WWTPs based on the measured results, which necessitates the development of a control strategy based on the effluent NH_4-N and NO_X-N concentrations. Finally, the developed control strategy or system including the control strategy should be applied in the field process without any additional tuning for a long time by excluding the need for complicated tools such as the use of mathematical models.

Our aim was to propose a real-time feedback control strategy based on hourly measurements of effluent NH_4-N and NO_X-N concentrations. Additionally, a control system was developed to operate two control strategies simultaneously in the target process. Because the overall structures of the control strategies were developed based on the measured effluent NH_4-N and NO_X-N concentrations, no additional nutrient sensors in the anoxic and aerobic reactors were required. Moreover, the manipulated variables for removal of NH_4-N and NO_X-N concentrations were divided in the control strategies and, therefore, the two different control strategies could be applied

†To whom correspondence should be addressed.
E-mail: cwkim@pusan.ac.kr

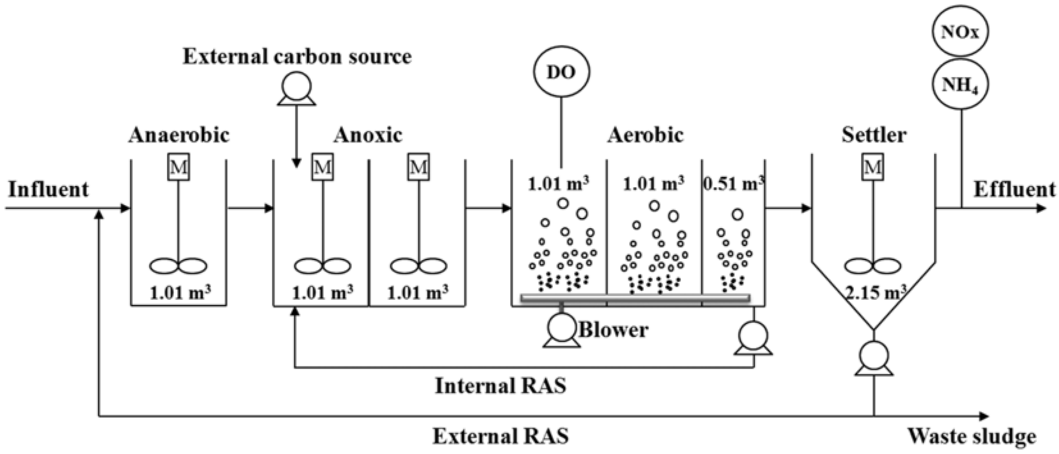

Fig. 1. Schematic diagram of the pilot-scale A^2/O process.

together. The proposed control system, including two real-time feedback control strategies, was tested on a pilot-scale A^2/O process of 18 m^3/day, and the results were evaluated in terms of the efficiency of the control strategies and the possibility of system application.

MATERIALS AND METHODS

1. Pilot-scale A^2/O Process

Fig. 1 shows a schematic diagram of the pilot-scale A^2/O process located on S WWTP (Busan, South Korea). The fixed influent flow rate of 18 m^3/day was fed into the pilot-scale A^2/O process. The hydraulic retention time and sludge retention time of biological reaction tanks in the operation range of the A^2/O process [9] were 7.5 hour and 10-15 days, respectively. The pilot-scale A^2/O process consists of an anaerobic reactor, two anoxic reactors, three aerobic reactors and a circular-type secondary settler. The design and operational conditions of the pilot-scale A^2/O process are shown in Table 1.

The default values of the external RAS flow rate and the internal RAS flow rate were operated at 50% and 200% of the influent flow rate, respectively. When the real-time feedback NH_4-N and NO_X-N control strategies were not applied in the pilot-scale A^2/O process, the air flow rate was operated at fixed rotational speed RPM and no external carbon source was fed into the pilot-scale A^2/O process.

Table 1. Design and operational conditions of the pilot-scale A^2/O process

Working volume (m^3)		Flow rate (m^3/d)	
Anaerobic reactor	1.01	Influent	18.0
Anoxic reactor	2.02	Internal RAS	31.0-52.0
Aerobic reactor	2.53	External RAS	9.0
Secondary settler	2.15	External carbon dose	0-0.085

When the real-time feedback NH_4-N and NO_X-N control strategies were applied in the pilot-scale A^2/O process, the air flow rate, internal RAS flow rate and external carbon dose flow rate were controlled according to each setpoint determined from the two control strategies. For the second and third aerobic reactors, each air flow rate was fed at about 50% and 30% of that of the first aerobic reactor by manipulating the valves manually. The DO concentration of the first aerobic reactor was measured at 10 second intervals, and the concentrations of NH_4-N and NO_X-N in the effluent were measured hourly using auto-analyzers (Monitor V, BLTEC Korea Co., Ltd., South Korea). The auto-analyzers were installed in the pilot-scale A^2/O process and utilized the reagents for data measurement.

2. Development of the Real-time Feedback NH_4-N Control Strategy

Based on the measured hourly effluent NH_4-N concentration from the auto-analyzers, a feedback NH_4-N control strategy of cascade type was developed to decide the DO setpoint in the first aerobic reactor. Olsson et al. [10] reported that the DO was the optimal manipulated variable for controlling the real-time NH_4-N concentrations. Kim et al. [11] showed that the sufficient removal of NH_4-N concentration could be maintained by using the DO setpoint except the other manipulated variables in the identical pilot-scale A^2/O process. Therefore, based on these results, we used the DO setpoint to control the effluent NH_4-N concentration.

Fig. 2 shows the control loop for the real-time feedback NH_4-N control strategy. First, the DO setpoint in the first aerobic reactor was decided by calculating the difference between the measured effluent NH_4-N concentration and the target NH_4-N concentration. Second, the proper air flow rate for maintaining the DO setpoint was fed into the first aerobic reactor by using a proportional integral derivative (PID) controller. Because the effluent NH_4-N concentration was measured hourly, the DO setpoint of the first aerobic reactor

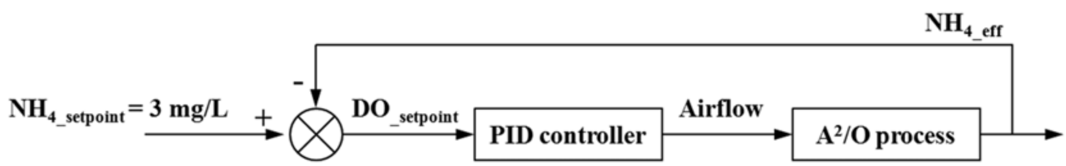

Fig. 2. Control loop based on the effluent NH_4-N concentration.

was also maintained at an identical value for 1 hour. The air flow rate was changed at about 10 second intervals according to the measured DO concentration in the first aerobic reactor.

To obtain the DO setpoint from the difference between the measured effluent NH_4-N concentration and the target NH_4-N concentration, Isaacs and Thornburg [12] used a stepwise-type function, which had the identical DO setpoint within the range of the defined concentration difference. Kim et al. [13] utilized the human operator's experience to deduce the DO setpoint, which increased or decreased the concentration difference proportionally. However, these calculations for DO setpoint were limited in that a fine change of the difference between the NH_4-N concentrations could not be applied and/or the proper DO setpoint could not be decided. To overcome these limitations, the sigmoid function of s-curve type [14] was selected in this study and modified within the range of the operational condition in the applied pilot-scale A^2/O process. The default type of sigmoid function is described by Eq. (1).

$$y = \frac{1}{1+\exp^{-x}} \tag{1}$$

For the DO setpoint in the range of the available DO concentration in the pilot-scale A^2/O process, Eq. (1) was modified to Eq. (2):

$$DO_{setpoint} = A + \frac{B}{1+\exp^{-C\times(NH_{4\_diff}-D)}} \tag{2}$$

where A is the offset, B is the scale, C is the gradient and D is the inflection.

For a small difference between the measured effluent NH_4-N and the target NH_4-N concentrations, the DO setpoint should be increased slightly, but increased rapidly in the case of a large difference. Therefore, each coefficient of the modified sigmoid function was manipulated to decide the proper DO setpoint value in the different range by using trial and error. Fig. 3 compares the stepwise and sigmoid types used in this study for deciding the DO setpoint.

As shown in the left side in Fig. 3, for the stepwise type, a higher DO setpoint value than that necessary might be deduced in a particular range. These results could be related to the excessive aeration. In contrast, for the sigmoid type used in this study, a fine change of the DO setpoint according to the value of NH_{4_diff} could be reflected, which enabled the optimal DO setpoint to be determined in the entire range. Table 2 lists the coefficients of the modified sigmoid function used for real-time feedback NH_4-N control.

Table 2. Coefficients of sigmoid function for calculating the DO setpoint and parameters of the PID controller

Sigmoid function		PID controller	
A (offset)	1.5	K_C	17.0
B (scale)	1.5	τ_I	0.6
C (gradient)	2.0	τ_D	1.2
D (inflection)	2.5	-	-

The PID controller could manipulate the air flow rate according to the deduced DO setpoint by using Eq. (3). The parameters of the PID controller were tuned from a pre-test in pilot-scale A^2/O process and each parameter value used for the real-time feedback NH_4-N control is listed in Table 2.

$$c(t) = c_0 + K_C \cdot \left[e(t) + \frac{1}{\tau_I} \cdot \int_0^t e(t)dt + \tau_D \cdot \frac{de(t)}{dt} \right] \tag{3}$$

where c_0 is the initial airflow rate, K_C is the proportional gain, e(t) is the difference between the DO setpoint and the measured DO, τ_I is the integral gain and τ_D is the derivative gain.

In South Korea, the legal discharge standard of the total nitrogen is 10 mg/L. Because the total nitrogen was the sum of the NH_4-N, NO_X-N and the organic nitrogen, in this study, the sum of the target effluent NH_4-N and NO_X-N concentrations was set to 8 mg/L to consider the part of the organic nitrogen in the effluent. Among these, the target NH_4-N concentration was set to 3 mg/L because the total volume of the aerobic reactors was 25% larger than that of the anoxic reactors. The change range of the air flow rate in the first aerobic reactor by the PID controller was set to 20-35 RPM.

3. Development of the Real-time Feedback NO_X-N Control Strategy

To effectively remove the NO_X-N concentration that occurs by the nitrification reaction in the aerobic reactor, the internal RAS flow rate according to the NO_X-N concentration should be increased proportionally. Moreover, when the C/N ratio of the influent is not enough, the additional external carbon source should be fed into the anoxic

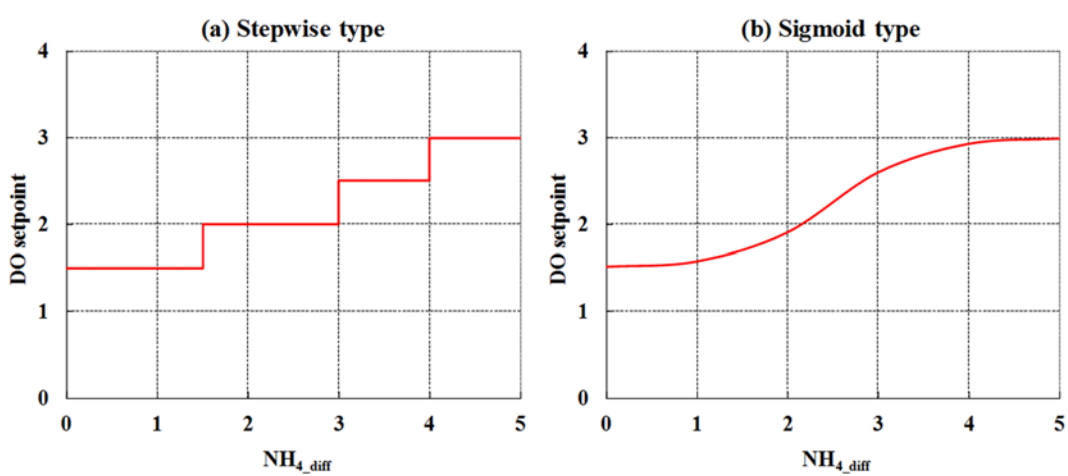

Fig. 3. Comparison of the stepwise type with the modified sigmoid function used for deducing the DO setpoint.

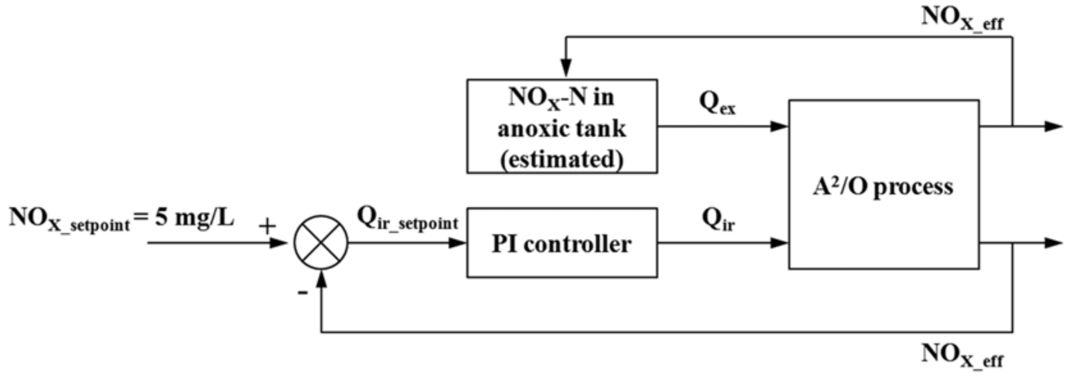

Fig. 4. Control loop based on effluent NO_X-N concentration.

reactor [10]. Because the C/N ratio of the influent which was fed into the pilot-scale A^2/O process was lower than 5, in this study, both the external carbon dose and internal RAS flow rate were used to control the effluent NO_X-N concentration. The real-time feedback NO_X-N control strategy was applied with two separate parts, as shown in Fig. 4. One part was used to calculate the external carbon dose flow rate based on the NO_X-N concentration in the anoxic reactor. The other part was used to set the target effluent NO_X-N concentration and control the internal RAS flow rate by using the PI controller.

We could not measure the NO_X-N concentration in the anoxic reactor directly because only the effluent NO_X-N concentration was measured hourly from the auto-analyzers. Therefore, the external carbon dose flow rate that was required to ensure sufficient denitrification could be calculated by determining the NO_X-N concentration in the anoxic reactor by using the effluent NO_X-N concentration. Because three flow rates, i.e., influent, internal and external RAS flow rates, were fed into the anoxic reactor, the empirical equation used to calculate the NO_X-N concentration in the anoxic reactor could be established based on a mass balance (Eq. (4)). The NO_X-N concentration in the influent flow rate was rare and was therefore omitted from Eq. (4).

$$NO_{X\_Anox} = \frac{[\alpha \cdot NO_{X\_eff} \cdot Q_{ir} + \beta \cdot NO_{X\_eff} \cdot Q_r]}{(Q_{inf} + Q_{ir} + Q_r)} \tag{4}$$

The used α and β values in Eq. (4) were decided by considering the operational state of the secondary settler and by using the trial and error method. The external carbon dose flow rate for denitrifi-

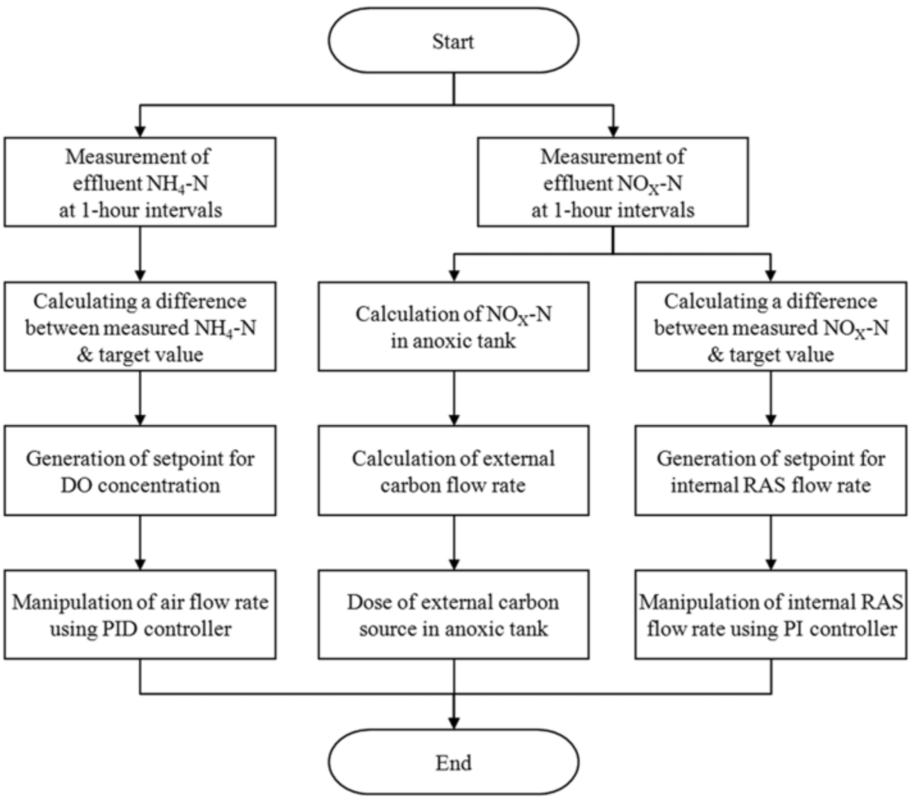

Fig. 5. Overall control flowchart for the real-time feedback NH_4-N and NO_X-N control strategies.

cation reaction was calculated by using the calculated NO_X-N concentration in the anoxic reactor (Eq. (5)). Because ethanol was selected as the external carbon source in this study, the loading rate of the COD equivalent was calculated based on the proper stoichiometric reaction. The microorganism yield suggested by Mokhayeri et al. [15] was used to calculate the loading rate of COD equivalent.

$$Q_{ex}=\frac{L}{C_{ethanol}}=\frac{\frac{NO_{X\_Anox}}{14}\cdot\frac{0.083}{0.095}\cdot 3\cdot 32\cdot(Q_{inf}+Q_{ir}+Q_r)}{12} \quad (5)$$

where L is the loading rate of COD equivalent (gCOD/day) and $C_{ethanol}$ is the COD equivalent of ethanol carbon source (gCOD/L).

For the control of the internal RAS flow rate according to the change of the effluent NO_X-N concentration, the aforementioned modified sigmoid function of s-curve type was used to find the setpoint of the internal RAS flow rate (Eq. (6)).

$$\text{Internal RAS}_{setpoint}=1.9+\frac{1.2}{1+\exp^{-1.0\times(NO_{X\_diff}-2.2)}} \quad (6)$$

The used function type was identical to Eq. (1). However, the NO_{X_diff} was used instead of NH_{4_diff}. According to the ratio of total volume between the aerobic and anoxic reactor, the target NO_X-N concentration was set to 5 mg/L.

4. Overall Control Flowchart and System Development

Fig. 5 shows the overall control flowchart for the proposed real-time feedback NH_4-N and NO_X-N control strategies. The left side of the flowchart presents the real-time feedback NH_4-N control strategy, which was used to control the air flow rate by using the measured hourly effluent NH_4-N concentration. The right two sides of the flowchart present the real-time feedback NO_X-N control strategy, which was used to dose the external carbon source and control the internal RAS flow rate by using the measured hourly effluent NO_X-N concentration.

In this study, an automatic control system had to be developed in order to apply the proposed control strategies hourly to the pilot-scale A^2/O process. Therefore, a control system that could implement the control flowchart of Fig. 5 was established with a user-friendly interface. When the effluent NH_4-N and NO_X-N concentrations were measured from the auto-analyzers, the proper control actions for nitrification and denitrification reactions through the control system were applied automatically in the pilot-scale A^2/O process. The control system was developed by using the LabVIEW program (ver. 8.6.1). All data signals were collected into the control system, and based on these data signals, the control system could calculate the setpoints and control the air flow rate of the first aerobic reactor, external carbon dose flow rate and internal RAS flow rate. As mentioned above, because the effluent NH_4-N and NO_X-N concentrations were measured hourly by auto-analyzers, the control actions through the automatic control system could be applied in the pilot-scale A^2/O process hourly.

RESULTS AND DISCUSSIONS

1. Application Results of the Real-time Feedback NH_4-N Control Strategy

Fig. 6 shows the results of the cases without control and with control by applying the real-time feedback NH_4-N control strategy. In 150-hr operation without control, a uniform air flow rate, 20 RPM, was supplied to the first aerobic reactor, and the average DO concentration was about 0.7 mg/L. The average influent and effluent NH_4-N concentrations and removal rate during these periods were about 27.4, 13.8 mg/L and 49.6%, respectively. On the other hand, in 50-hr operation with control, the air flow rate was changed in the range of 20-35 RPM by applying the PID controller, and the average DO concentration was about 1.6 mg/L. The average influent and effluent NH_4-N concentrations and removal rate during these periods were about 19.7, 1.3 mg/L and 93.4%, respectively.

When the real-time feedback NH_4-N control strategy was not applied in the pilot-scale A^2/O process, the air flow rate supplied to the aerobic reactors was insufficient for stable nitrification reaction. This caused high effluent NH_4-N concentration during the period without control. On the other hand, when a control action was applied in the pilot-scale A^2/O process, the proper DO setpoint that required nitrification reaction could be determined and the air flow rate required for nitrification reaction was supplied to the first aerobic reactor continuously. This result confirmed that an effluent NH_4-N

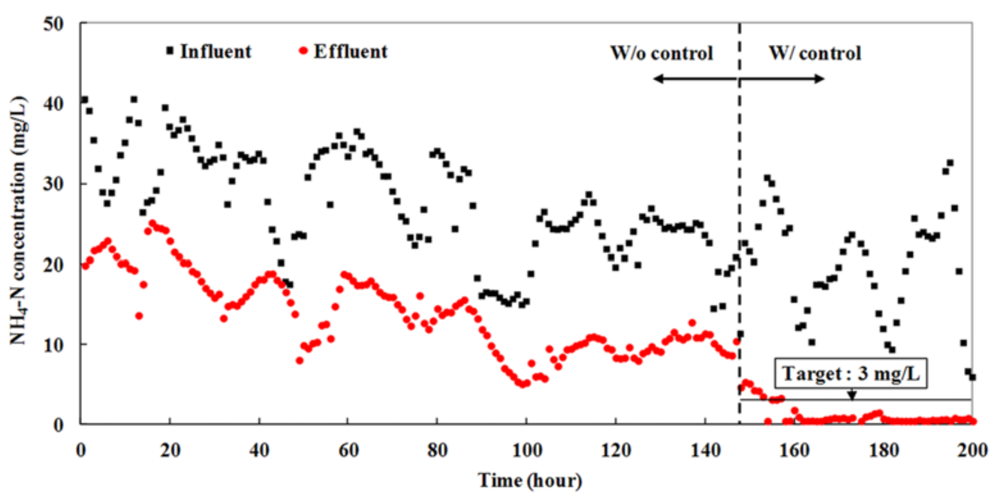

Fig. 6. Results of without control case and with control case by applying real-time feedback NH_4-N control strategy (without control and with control mean without control strategy and with control strategy, respectively).

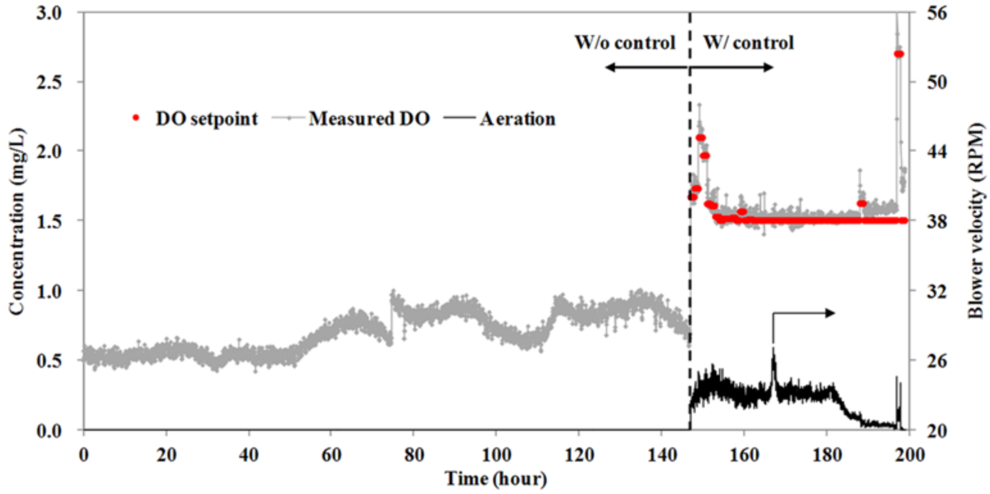

Fig. 7. DO setpoints, measured DO and air flow rate during non-control periods and the application periods of the real-time NH_4-N control strategy.

concentration lower than the target NH_4-N concentration of 3 mg/L could be maintained stably, as shown in Fig. 6.

From the result of the control application during about 160-200 hr, the average effluent NH_4-N concentration of about 1 mg/L, which was lower than the target value of 3 mg/L, occurred. This was because the aeration strength of the second and third aerobic reactors was increased. In the pilot-scale A^2/O process, only one blower was used and the aeration strength of each aerobic reactor was maintained by manipulating the valve manually. Therefore, when the air flow rate was increased to maintain the DO setpoint of the first aerobic reactor, the aeration of the second and third aerobic reactors also was increased. In the cases of use of each blower or automatic valve in each aerobic reactor, it is expected that the effluent NH_4-N concentrations which are close to the target value of 3 mg/L are maintained.

Fig. 7 shows the DO setpoints, measured DO and air flow rate during the non-control periods and the application periods of the real-time NH_4-N control strategy. As shown in Fig. 7, the DO setpoints in the first aerobic reactor during the control period were changed hourly according to the difference between the measured effluent NH_4-N concentration and the target NH_4-N concentration. Additionally, the measured DO concentration, which was similar to the set DO concentration, was maintained by changing the air flow rate by the PID controller. The average air flow rate during the 50-hr control period was about 22.5 RPM, which was only increased by 12.5% compared to that during the non-control period.

These results identified that a sufficient DO concentration for nitrification reaction in the first aerobic reactor could be calculated by using the proposed real-time feedback NH_4-N control strategy based on the effluent NH_4-N concentration. In addition, because the modified sigmoid function, which could deduce the optimal DO setpoint according to the concentration difference, was used with the control strategy, an effluent NH_4-N concentration lower than the target NH_4-N concentration could be maintained without having to supply an unnecessarily high air flow rate.

2. Application Results of the Real-time Feedback NO_X-N Control Strategy

The α and β values in the empirical equation based on mass balance for determining the NO_X-N concentration in the anoxic reactor had a significant effect on the result of the equation. Because the NO_X-N concentration that was used in the empirical equation was measured in the effluent, the operational state of the secondary settler should be considered for determining the correct α and β values. The bulking phenomenon, which is an indication of rising sludge in the secondary settler, was identified during the entire test period. Therefore, the NO_X-N concentration in the effluent was expected to be higher than that in the aerobic reactor. Thus, the α value, which means the determined coefficient of NO_X-N concentration in the internal RAS flow rate, was lower value than 1. Additionally, the NO_X-N concentration of the lower part in the secondary settler was expected to be similar to that in the effluent. Thus, the β value, which means the determined coefficient of NO_X-N concentration in the RAS flow rate, was near 1. Based on these expectations, the optimal α and β values could be found by trial and error. The calculated α and β values were 0.5976 and 0.9026, respectively. Fig. 8 compares the measured NO_X-N concentration in the anoxic reactor and that calculated by using the empirical equation.

Fig. 8 confirms that the proper α and β values for considering the operational state of secondary settler were found to describe the behavior of the measured NO_X-N concentration in the anoxic reactor. For a more quantitative analysis, the root mean square error (RMSE) between the measured NO_X-N concentration and the calculated NO_X-N concentration was calculated by using Eq. (7). The result of about 0.74 revealed a relatively small difference, which indicated that the NO_X-N concentration in the anoxic reactor could be accurately estimated by using the empirical equation.

$$\mathrm{RMSE}=\sqrt{\frac{1}{\mathrm{N}-1}\cdot\sum_{i=1}^{N}(\mathrm{X}_{m,i}-\mathrm{X}_{p,i})^2} \tag{7}$$

where N is the total number of datasets compared, $X_{m,i}$ is the i^{th} measured value, and $X_{p,i}$ is the i^{th} predicted value.

The setpoint of the internal RAS flow rate was increased gradually in the entire range of the difference between the target NO_X-N concentration and the measured NO_X-N concentration in the effluent, against the case of the determination of the DO setpoint. Parame-

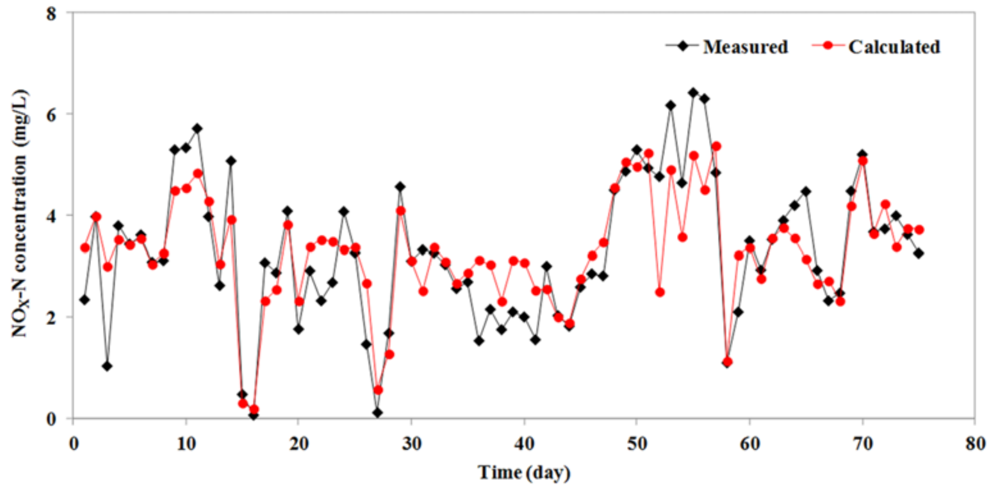

Fig. 8. Comparison of the measured NO_X-N concentration in the anoxic reactor and that calculated by using the empirical equation.

ters of PI controller for manipulating the internal RAS flow rate were tuned by using the trial and error in pilot-scale A^2/O process in advance. As a result, the values of the proportional and integral gain were 5.0 and 3.0, respectively. The tuned parameters of PI and PID controller in this study were based on the trial and error method; however, it could be considered that the proper tuning approach was applied in the pilot-scale A^2/O process because the empirical knowledge for process operation was combined with the trial and error method. To maintain more efficient control performance, a series of tuning processes should be repeated consistently according to the constant period.

Fig. 9 shows the results of the case without control and with control by applying the real-time feedback NO_X-N control strategy. During the 150-hr non-control period, the external carbon source was not fed into the anoxic reactor. On the other hand, during the 50-hr control period, the external carbon source was fed by using the calculated NO_X-N concentration in the anoxic reactor and Eq. (5).

Because the real-time feedback control strategy for sufficient nitrification reaction was not applied during the non-control periods, the NO_X-N concentration in the effluent was also maintained in a low range. After about 150 hours, the real-time feedback NH_4-N control strategy was applied and sufficient nitrification reaction was maintained continuously. This was expected to increase the NO_X-N concentration in the effluent. However, the real-time feedback NO_X-N control strategy was applied simultaneously during these control periods and sufficient external carbon sources for denitrification reaction were fed into the anoxic reactor. This confirmed that the effluent NO_X-N concentration could be maintained below the target NO_X-N concentration of 5 mg/L. During the 150-hr non-control and 50-hr control periods, the average effluent NO_X-N concentrations were about 3.8 and 2.9 mg/L, respectively. From these results, through application of the real-time feedback NO_X-N control strategy, an external carbon dose flow rate sufficient to remove the NO_X-N concentration generated from nitrification reaction in the aerobic reactor, and the secondary settler could be calculated. Additionally, we confirmed that sufficient external carbon source was fed into the anoxic reactor hourly and that the denitrification reaction in the anoxic reactor was maintained properly.

Fig. 10 shows the flow rates of the external carbon dose and internal RAS during the control period. The external carbon dose flow

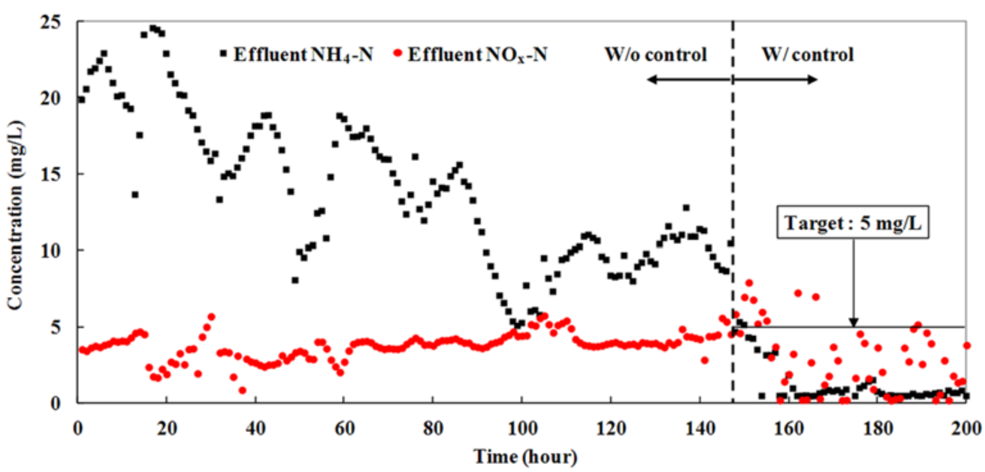

Fig. 9. Results of without control case and with control case by applying the real-time feedback NO_X-N control strategy.

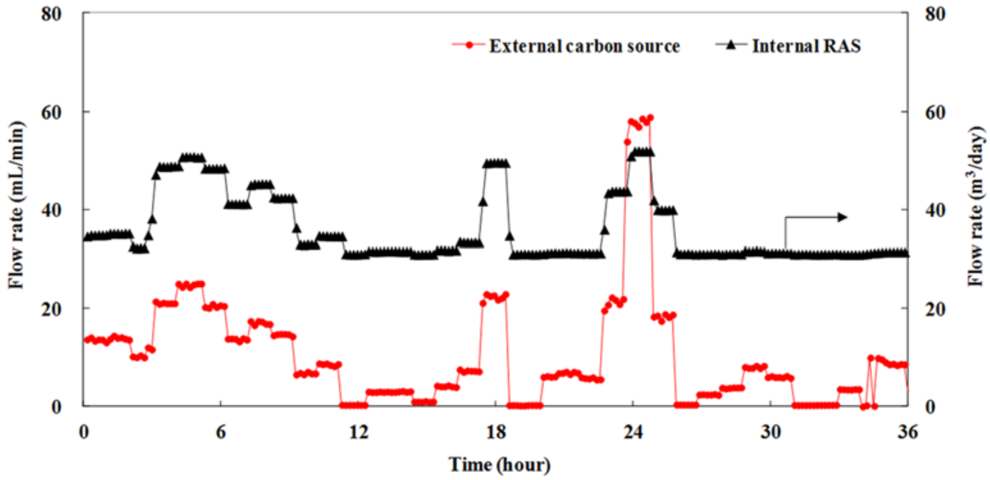

Fig. 10. Flow rates of external carbon dose and internal RAS during the application period of the real-time NO_X-N control strategy.

rate required for sufficient denitrification reaction could be calculated hourly by using Eqs. (4) and (5). In addition, the internal RAS flow rate could be changed hourly according to the difference between the target NO_X-N concentration and the measured NO_X-N concentration in the effluent.

These results confirmed that the NO_X-N concentration in the anoxic reactor could be determined by applying the real-time feedback NO_X-N control strategy proposed in this study. Moreover, the external carbon source for the denitrification reaction could be fed properly

Table 3. Mean air flow rate, external carbon flow rate and effluent concentrations in the cases of with and without control

Subject	With control	Without control
Air flow rate (RPM)	22.5	20.0
External carbon flow rate (mL/min)	10.4	0
Effluent NH_4-N (mg/L)	1.3	13.8
Effluent NO_X-N (mg/L)	2.9	3.8

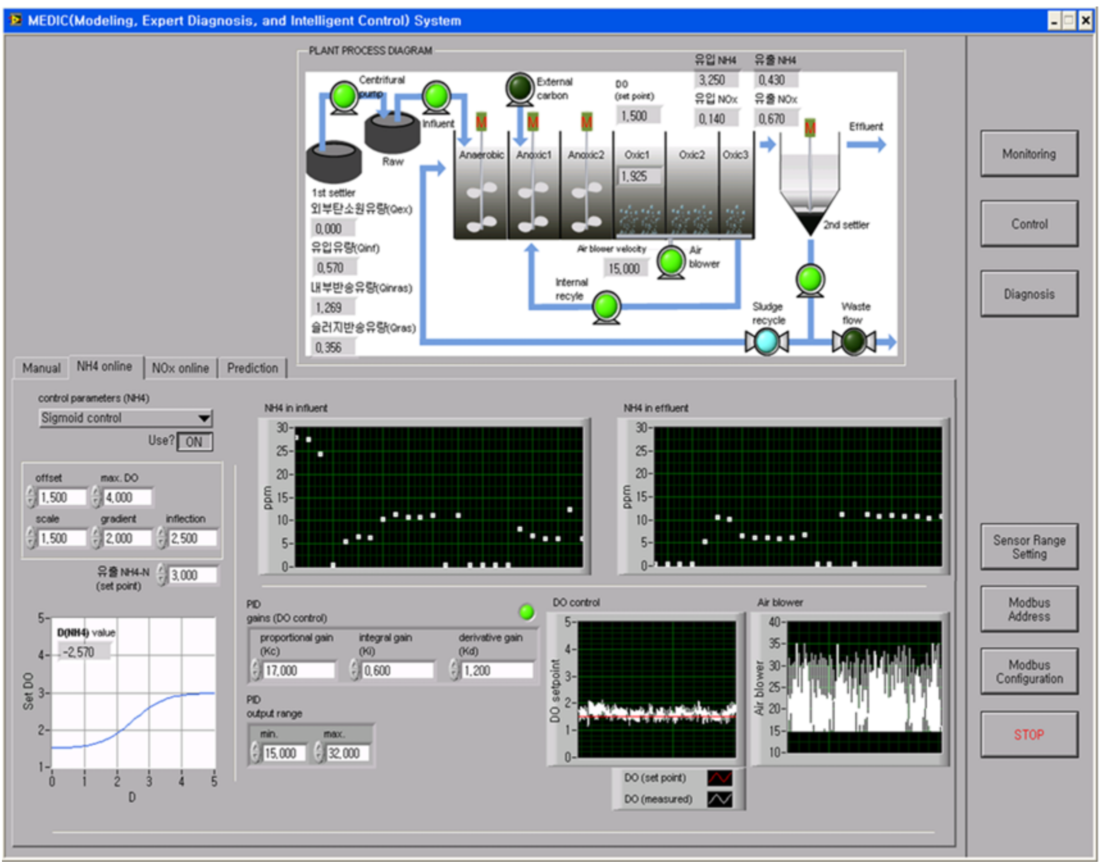

Fig. 11. System picture for the real-time feedback NH_4-N control strategy.

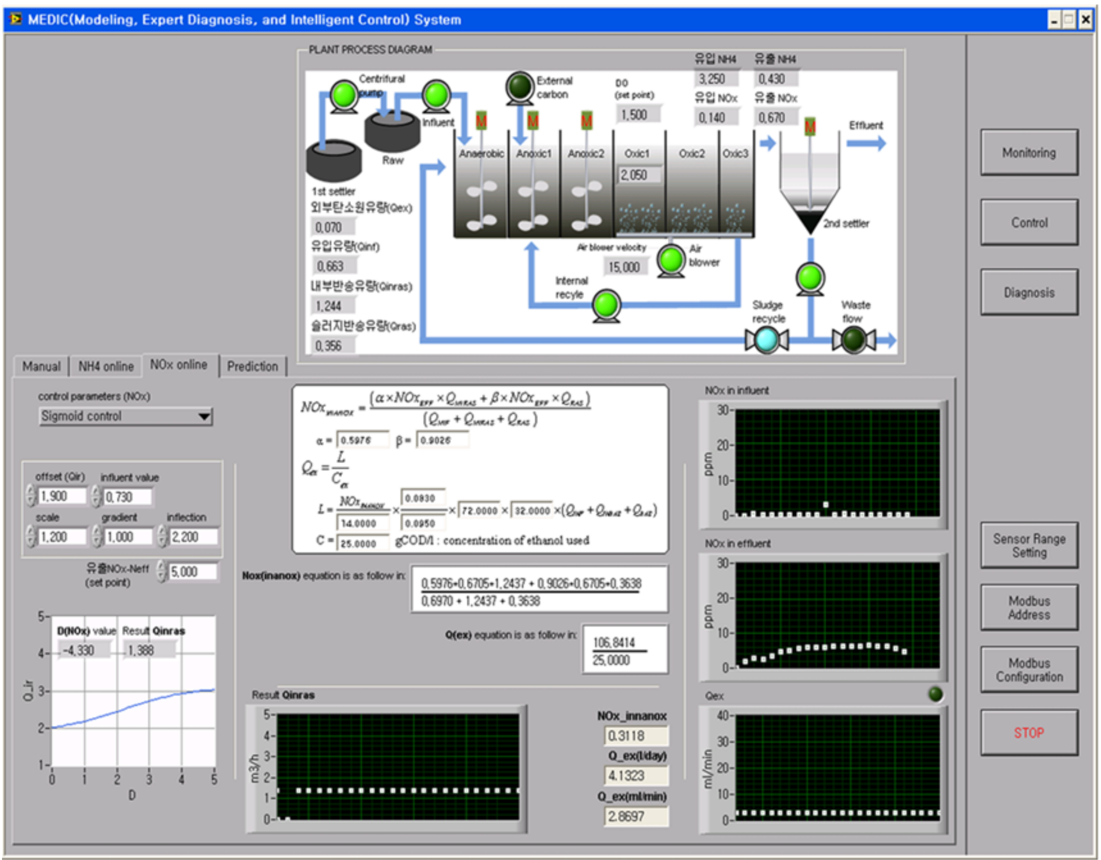

Fig. 12. System picture for the real-time feedback NO_X-N control strategy.

based on the proper stoichiometric reaction, and the internal RAS flow rate could be simultaneously manipulated to set target NO_X-N concentration. As a result, despite the increased NO_X-N concentration corresponding to sufficient nitrification reaction, the effluent NO_X-N concentration could be stably maintained lower than the target NO_X-N concentration. Table 3 lists the average air flow rate, external carbon dose flow rate and effluent NH_4-N and NO_X-N concentrations in the non-control case with simultaneous application of the real-time feedback NH_4-N and NO_X-N control strategies.

The overall control strategies and system suggested in this study were established based on auto-analyzers that could measure the effluent NH_4-N and NO_X-N concentration hourly. The application interval of real-time control can differ according to the time needed for measurement. When the real-time control strategy is applied for a relatively short interval, the target process might be operated more effectively. However, various conditions such as sufficient time for reaction, duplication utilization of the manipulated variable and complexity of the control strategy should be considered. The real-time feedback NH_4-N and NO_X-N control strategies developed in this study used different manipulated variables and developed as relatively simple driven flow. Therefore, in the case of a short measurement interval, unlike in this study, the two proposed control strategies can be applied in the target field plant while maintaining stable operation performance for a long time.

3. System Development for the Real-time Feedback NH_4-N and NO_X-N Control Strategies

Fig. 11 shows a system picture of the real-time feedback NH_4-N control strategy developed in this study. The top part of the picture presents a schematic diagram of the pilot-scale A^2/O process. The bottom left of the picture presents the coefficients of the modified sigmoid function and the DO setpoint graph, which was determined according to the difference between the measured NH_4-N concentration in the effluent and the target NH_4-N concentration. The graphs in the bottom right of the picture identify the changes of air flow rate and the measured NH_4-N concentration.

Fig. 12 shows a system picture of the developed real-time feedback NO_X-N control strategy. The bottom left of the picture presents the coefficients of the modified sigmoid function and the setpoint graph of the internal RAS flow rate, which was decided according to the difference between the measured NO_X-N concentration in the effluent and the target NO_X-N concentration. The center part presents the equations for finding the NO_X-N concentration in the anoxic reactor and for calculating the external carbon dose flow rate. The bottom right of the picture presents the graphs for measuring the NO_X-N concentration in the effluent and for the external carbon dose flow rate.

CONCLUSION

Two real-time feedback control strategies based on the measured effluent NH_4-N and NO_X-N concentrations were proposed, and a control system that included the two proposed control strategies was developed for controlling the pilot-scale A^2/O process automatically. A field test revealed that the effluent NH_4-N and NO_X-N concentrations were maintained stably below the target values by applying the proposed real-time feedback NH_4-N and NO_X-N control strategies.

The real-time feedback NH_4-N control strategy was developed by selecting a cascade-type control structure capable of determining the DO setpoint value based on the difference between the measured effluent NH_4-N and the target NH_4-N concentrations. The modified sigmoid function of the s-curve type was used to decide the DO setpoint value. Application of the modified sigmoid function enabled the optimal DO setpoint, which could reflect the fine change of the difference between the measured effluent NH_4-N and the target NH_4-N concentrations to be determined over the entire range.

For the real-time feedback NO_X-N control strategy, the NO_X-N concentration in the anoxic reactor was determined by using the empirical equation based on mass balance. The availability of empirical equations such as developed in this study will be increased with the accumulation of more measured operational data. Additionally, the empirical equation used had to be periodically calibrated and validated at regular intervals.

ACKNOWLEDGEMENTS

This research was supported by Korea Ministry of Environment as The Eco-innovation project. This study was also financially supported by the 2013 Post-Doc. Development Program of Pusan National University.

NOMENCLATURE

α : deduced coefficient of the NO_X-N concentration in the internal RAS flow rate
β : deduced coefficient of the NO_X-N concentration in the external RAS flow rate
A^2/O : anaerobic/anoxic/oxic
DO : dissolved oxygen
NH_{4_diff} : difference between the target NH_4-N concentration and the measured NH_4-N concentration in the effluent
NH_{4_eff} : measured effluent NH_4-N concentration
NO_{X_diff} : difference between the target NO_X-N concentration and the measured NO_X-N concentration in the effluent
NO_{X_eff} : measured effluent NO_X-N concentration
Q_{ex} : external carbon dose flow rate
Q_{inf} : influent flow rate
Q_{ir} : internal RAS flow rate
Q_r : external RAS flow rate
RAS : recycle activated sludge
RPM : revolution per minute
WWTP : wastewater treatment plant

REFERENCES

1. E.-T. Lim, G.-T. Jeong, S.-H. Bhang, S.-H. Park and D.-H. Park, *Bioresour. Technol.*, **100**, 6149 (2009).
2. P. Ingildsen, U. Jeppsson and G. Olsson, *Water Sci. Technol.*, **45**(4-5), 453 (2002).
3. K. Krause, K. Böcker and J. Londong, *Water Sci. Technol.*, **45**(4-5), 413 (2002).
4. D. Vrečko, N. Hvala, A. Stare, O. Burica, M. Stražar, M. Levstek, P. Cerar and S. Podbevšek, *Water Sci. Technol.*, **53**(4-5), 125 (2006).
5. J. A. Baeza, D. Gabriel and J. Lafuente, *Water Res.*, **36**, 2109 (2002).
6. J.-H. Cho, S. W. Sung and I.-B. Lee, *Water Sci. Technol.*, **45**(4-5), 53 (2002).
7. M. Ekman, P. Samuelsson and B. Carlsson, *Water Sci. Technol.*, **47**(11), 137 (2003).
8. P. Samuelsson and B. Carlsson, *Water Sci. Technol.*, **43**(1), 115 (2001).
9. P. A. Vesilind, *Wastewater treatment plant design*, Water Environment Federation, USA (2003).
10. G. Olsson, M. Nielsen, Z. Yuan, A. Lynggaard-Jensen and J. P. Steyer, *Instrumentation, control and automation in wastewater systems*, IWA Publishing, UK (2005).
11. H. S. Kim, Y. J. Kim, S. P. Cheon, G. D. Baek, S. S. Kim and C. W. Kim, *Chem. Eng. J.*, **203**, 387 (2012).
12. S. Isaacs and D. Thornberg, *Water Sci. Technol.*, **38**(3), 281 (1998).
13. H. Kim, Y. Kim, J. Cha, K. Min, J. Gee and C. Kim, *Water Sci. Technol.*, **60**(4), 879 (2009).
14. D. E. Wachenheim, J. A. Patterson and M. R. Ladisch, *Bioresour. Technol.*, **86**, 157 (2003).
15. Y. Mokhayeri, R. Riffat, I. Takacs, P. Dold, C. Bott, J. Hinojosa, W. Bailey and S. Murthy, *Water Sci. Technol.*, **58**(1), 233 (2008).